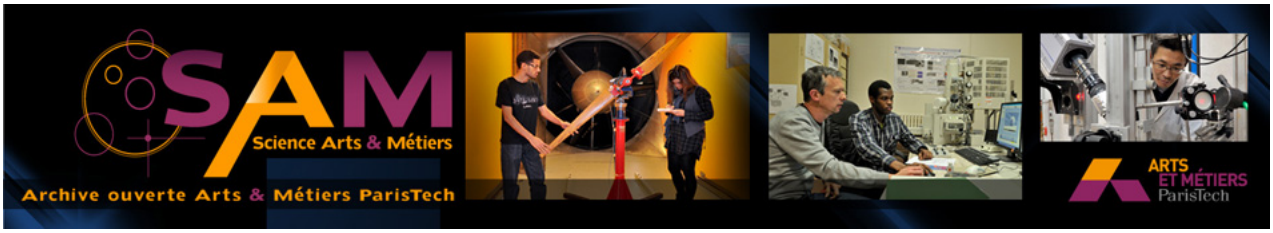

Multiscale functional analysis of wear
A fractal model of the grinding process

M. Bigerelle[a,b,*], D. Najjar[b], A. Iost[b]

[a] *Laboratoire Roberval, FRE 2833, UTC/CNRS, Centre de Recherches de Royallieu, BP20529, 60205 Compi`egne, France* [b] *ESI, LMPGM UMR CNRS 8517, ENSAM Lille, 8 boulevard Louis XIV, 59046 LILLE, Cedex, France*

Abstract

In this paper, we propose to create a fractal function defined by an infinite series to model worn surfaces obtained by a grinding process. In this series, each elementary term characterizes a wear process at a given scale. This series is only defined by two parameters: an amplitude parameter and the fractal dimension. This model is tested on worn profiles obtained by using different grinding paper grades and roughness is assessed by tactile profilometry. Then an inverse method is developed to obtain simulated profiles that present the same morphology as the experimental ones. The results from this study prove that our method allows simulation of profiles with elementary functions that characterize the wear process.

Keywords: Wear; Roughness; Profilometry; Simulation; Smoothing effect

1. Introduction

Roughness is of much importance in surface response in relation to mechanical or physical solicitations. An important concept is to construct an analytical description that well represents the original topography of the surface. Then it becomes possible to perform some analytical calculi on this surface, i.e. parameter estimations, boundary conditions on differential equations, etc. There is a high number of signal transforms that allows us to model the surface, such as the Fourier transform, the Haar and Hilbert ones, etc. and more recently the wavelet transform. All these transforms suppose that the surface can be represented by an infinite (or finite for discretized profiles) number of elementary functions (cosines, rectangle, Gaussian, etc.). However, do these elementary functions possess a physical sense with regard to the observed phenomena? It is true for periodic acoustic signals; the Fourier transform possesses some physical sense because the solution to a wave equation is often a series of sinus functions. However, it becomes risky to postulate that the formation of a machined surface can be explained by a superposition of sinus functions. If so, elementary functions must model the basic principle of the creation of the surface topography and include its fractal properties (as a high number of surfaces possess fractal properties [1–8]). Since Mandelbrot's works [9,10], it has been shown that numerous classes of surfaces cannot be modeled with derivative functions and then are nowhere derivative [11–14]. These surfaces are called fractals and all metric parameters built on these surfaces depend on the measurement scale. The fractal properties imply that between two adjacent points of the surface, however close they are, the curves cannot be seen as increasing or decreasing. A method intensively used to simulate fractal surfaces is the Fractional Brownian Motion [15,16]. However, this method involves restriction of the mathematical properties of the surfaces (like self affinity). Moreover, some artifacts in the Fast Fourier Transform make this method uncertain: this theory supposes that the spectrum of the surface follows the power law $P(f) \propto f^{2\Delta-5}$ and highest frequency $f_h \gg 1/L$, where L is the scanning length [16,17].

* Corresponding author. Tel.: +33 344 234 423; fax: +33 344 235 284.
E-mail address: maxence.bigerelle@utc.fr (M. Bigerelle).

Nomenclature

a	regression slope of $\log P(f)$ versus $\log f$
A	scaling amplitude factor
f	frequency of the power spectrum
f_h	highest calculated frequency of the power spectrum
F_{CF}	circle function
F_{MSCF}	Stochastic circle function with added terms
F_{SCF}	Stochastic circle function
g	elementary function of period 1 defined on [0, . . ., 1]
$\Delta(G_f)$	fractal dimension associated to the graph of the function f
H	Hölder exponent
l_x	characteristic length for local peak radius curvature computation (see Appendix C)
l_y	characteristic height for local peak radius curvature computation (see Appendix C)
L	scanning length of profiles
p	integer higher than unity
$P(f)$	power spectrum
r_c	local peak radius curvature (see appendix C)
W	Weierstrass function
x	abscissa of the profile

Greek letters

α	angle to define different g function
β	amplitude scaling factor
ϕ_n	Gaussian random numbers
γ	frequency parameter greater than unity
φ_n	uniform random numbers
Ψ_n	positive Gaussian random numbers

Terms

ANAM	average normalized autocorrelation method
CF	circle function
d.f.	degree of freedom
D	fractal dimension calculated by ANAM
F	Fisher value
MS	mean square
p_c	critical value of a statistical test
PDS	power density spectrum
peaks	number of peaks per inch of profiles
Ra	mean roughness amplitude
Rt	range amplitude
WF	Weierstrass function

Furthermore, it must be borne in mind that all experimental devices involve a certain amount of smoothing or degradation of the real surface [18–22]. As the smoothing effect is highly non-linear, it becomes very hard to estimate the effect of smoothing on the original data. However, it remains of paramount importance to quantify the scale where the smoothing effect plays a role.

The aim of this paper is to define an analytical model of the topography of a surface taking into account the microscopic features of the elementary wear process at a given scale and amplitude (i.e. the shape of the grooves generated by a grain of silicon carbide during the grinding process of the surface of an aluminum sheet is investigated here). Based on the concept of fractal geometry, a mathematical summation of several elementary processes at different scales and amplitudes is used to generate final simulated profile that look like the experimental one recorded by tactile profilometry. Furthermore, on these modeled profile, a simulation of a mechanical scanning is applied to analyze and quantify the scale on which the smoothing effect must be considered.

2. Analytical model: the Fractal circle function

The aim of this chapter is to create a new fractal function that describes the grinding process. We shall assume that grains of silicon carbide of the grinding papers have approximately a hemispherical shape. We shall then assume that the scratches can be seen as indentations having a circular shape which follows a power law. As a consequence, the profile is described as a sum of elementary half-circles. The basic idea is to show that a high number of ground profiles looks like the graph of this function.

Let us first define an elementary function $g(x)$ of period 1 on the [0, . . ., 1] interval as follows:

$$g(x) = \sqrt{0.5^2 - (x - 0.5)^2} \quad x \in [0, \ldots, 1] \tag{1}$$

We then propose the deterministic Fractal circle function (Fig. 1):

$$F_{CF}(x) = A \sum_{n=0}^{\infty} 2^{-nH} g(2^n x) \tag{2}$$

where $H \in [0, \ldots, 1]$ and A is a scaling amplitude factor.

Theorem. The fractal dimension of the profile $\Delta(G_f)$ is given by:

$$\Delta(G_f) = 2 - H \tag{3}$$

To take into account the stochastic component of experimental profiles, a stochastic version of the previous function given by Eq. (2) (Fig. 2) must be formulated:

$$F_{SCF}(x) = A \sum_{n=0}^{\infty} \Psi_n 2^{-nH} g(2^n x + \varphi_n) \tag{4}$$

where Ψ_n are positive Gaussian random numbers that physically represent the stochastic variation of stress during the grinding process, and φ_n are uniform random numbers that represent the disorientation of the grooves due to the rotation

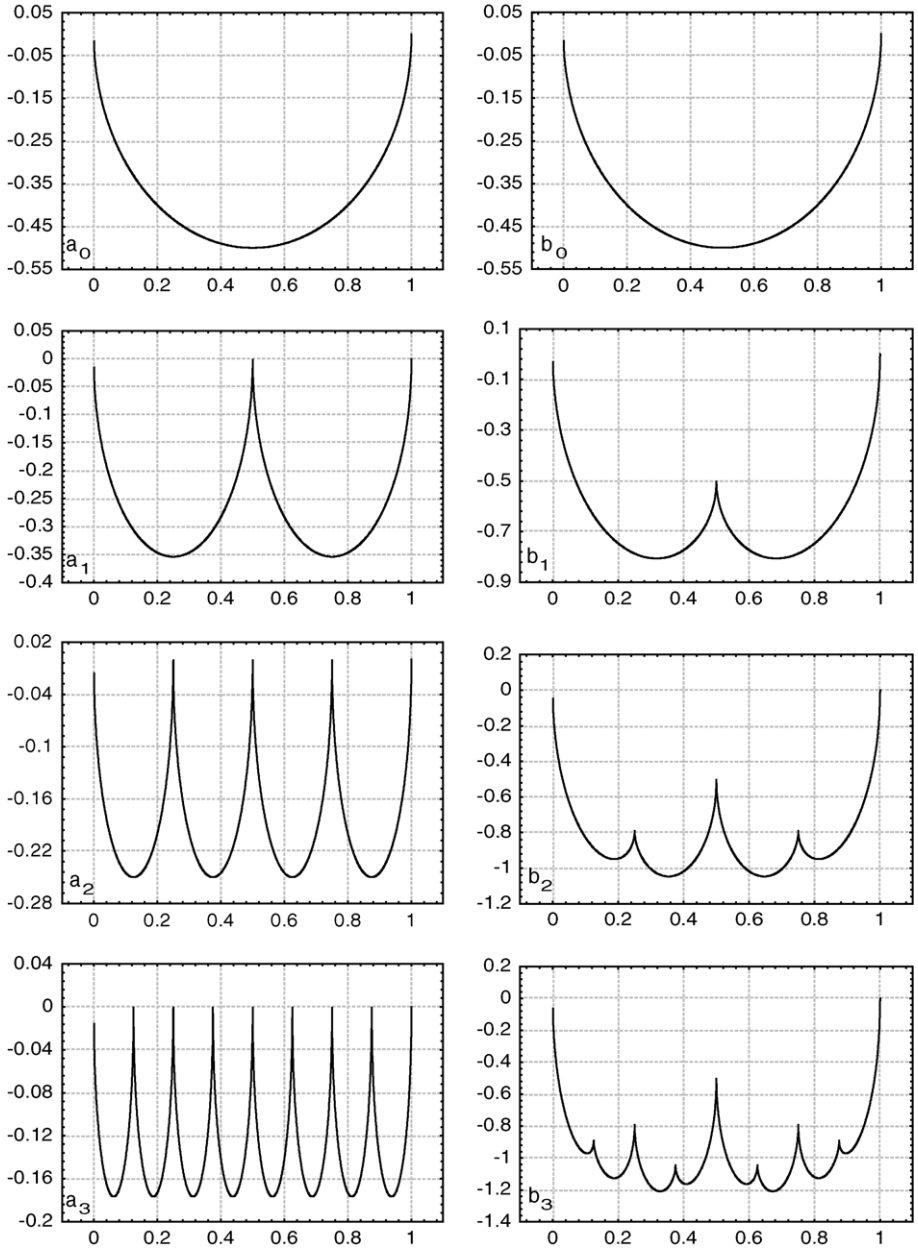

Fig. 1. Fractal circle function: (a_0–a_3) represent $g(2^0x)$, . . ., $g(2^3x)$ and (b_0–b_3) $\sum_{n=0}^{0} 2^{-n/2} g(2^n x)$, . . . , $\sum_{n=0}^{3} 2^{-n/2} g(2^n x)$.

of the grinding disk. These numbers leave the fractal dimension unchanged. In fact, Ψ_n-values allow us to moderate the perfect circle hypotheses of the g function. An analysis reported in Appendix A proves that taking a quarter of a circle rather a half to define the g functions does not change the amplitude parameters such Ra or the frequency ones, such as the number of peaks and this is confirmed for any fractal dimension $\Delta(G_f)$.

Only a few terms are needed to discretize the curve because of the exponential decrease in the period in the $g(x)$ function. For $n = 0$, the function is defined on [0, . . ., 1], $n = 1$ on [0, . . ., 0.5], $n = 2$ on [0, . . ., 0.25] and so on. This means that very quickly the period of the function will reach the sampling length. Consequently, the shape of elementary functions will often appear on the graph of $F_{SCF}(x)$. To avoid this numerical fact, we have to add new terms to the fractal series without modifying the fractal dimension. We then retain the new function:

$$F_{MSCF}(x, p) = A \sum_{n=0}^{\infty} \Psi_n 2^{-(nH/p)} g(2^{n/p} x + \varphi_n) \qquad (5)$$

with p an integer higher than unity.

As a consequence, the spectrum of the function Eq. (5) tends to be more continuous than those described in the literature [23]. It must be outlined that these non-integer indicia

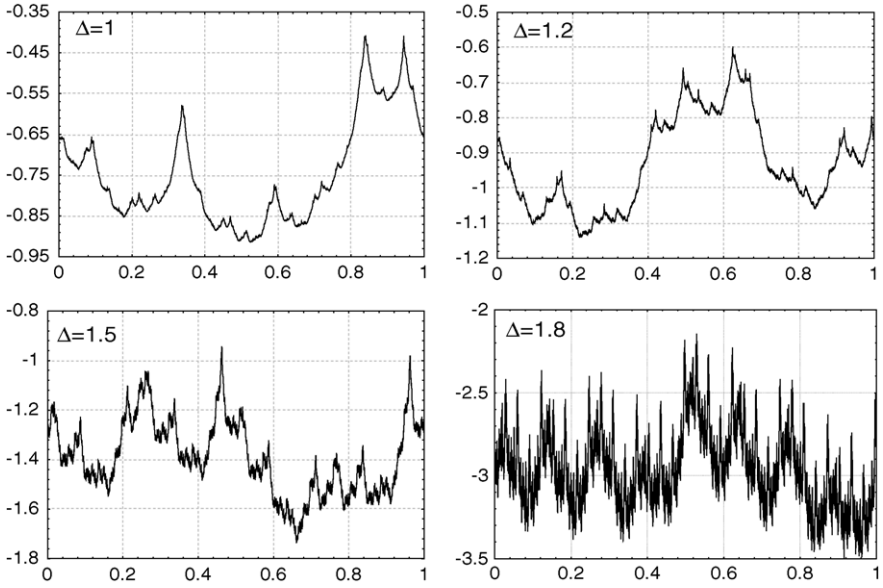

Fig. 2. Stochastic circle function with four fractal dimensions corresponding to $H \in \{1, 0.8, 0.5, 0.2\}$.

(n/p) can be introduced for any fractal function described by series, such as the Knopp function [12]. It becomes obvious to compare the efficiency of our function with the conventional Weierstrass one because of frequent use in the profile roughness modeling. By spectrum analyses, it is shown that our circle function gets a more continuous spectrum which better corresponds to the grinding process (see Appendix B). The use of Eq. (5) to model profiles allows us to estimate more efficiently the numerical fractal determination of simulated profiles.

3. Study of worn surfaces

3.1. Analyses of experimental profiles

A pure aluminum sheet was ground with paper grade 500. Then 30 profiles were recorded using a tactile profilometer with a stylus radius of 10 μm. Fig. 3a shows an example of a ground profile with paper grade 500. Fig. 4 shows the variation of the local peak radius curvature $\log r_c(l_x)$ versus $\log l_x$ (see Appendix C for the definition of the local peak radius curvature $r_c(l_x)$). As can be observed in this figure, a cross-over appears around $r_c(l_x) = 10$ μm. Under this critical value, $r_c(l_x)$ seems to be constant and over this value, $r_c(l_x)$ follows the power law given by Eq. (C1).

3.2. Simulation of worn profiles

It can be noticed that only two parameters have to be determined for the definition of the Fractal circle function proposed in this paper: the amplitude factor A and the Hölder exponents H. The p-value is chosen to be high enough ($p = 10$) so as to avoid statistical artifact in the spectrum representa-

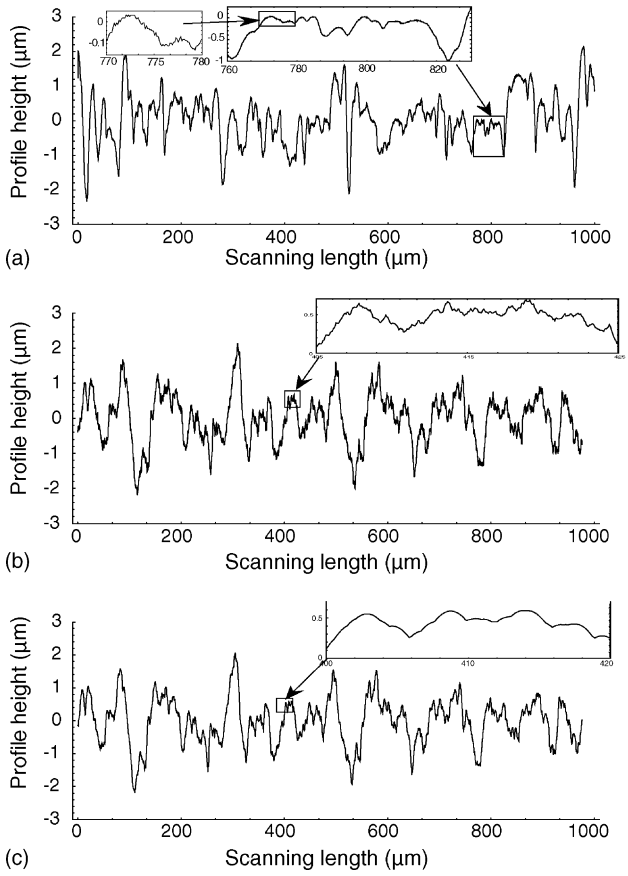

Fig. 3. (a) Profile of a pure aluminum sheet surface (ground with grain size 500) recorded by means of a tactile profilometer with a stylus radius of 10 μm. (b) Simulation of a profile by Stochastic circle function. (c) Simulation of the scanning of the profile (b) considering a stylus radius of 10 μm.

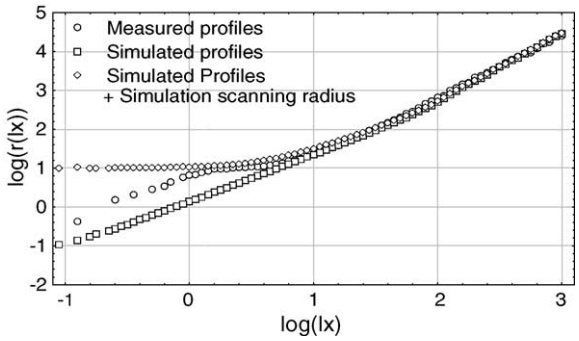

Fig. 4. Evolution of the peak radius curvature $\log r(l_x)$ vs. $\log l_x$ for profiles shown in Fig. 3a and c.

tion. To calculate the pair (H, A), we have to discuss the properties of the fractal peak radius curvature. According to Eq. (C1), if the profile is scaled in amplitude by a factor β, then $r_c(l_x) = l_x^2/8\beta l_y$ and finally in log–log representation of $\log r_c$ versus $\log l_x$, the curves decrease vertically to a value of $\log \beta$. If H changes to H', the fractal dimension changes from $\Delta(G_f) = 2 - H$ to $\Delta(G_f) = 2 - H'$ and as a consequence from Eq. (C2), the slope of $\log r_c(lx)$ versus $\log l_x$ changes too. Then the slope of this graph related to the experimental profiles is estimated to obtain the H exponent. To calculate A, the simulated curve is plotted by taking $A = 1$ with the value of H firstly estimated. Finally, the A-value is deduced by analyzing the vertical difference between simulated curves and experimental curves. Fig. 4 represents the log–log graph of both the experimental and the simulated evolutions of the fractal peak radius curvature versus the evaluation length.

3.3. *Smoothing effect of the stylus radius*

The basic idea we shall develop is to apply the theory of the fractal peak radius curvature of the profile to detect the scale where the measurement system introduces a smoothing effect on data measurement. In fact, the smoothing effect will increase the fractal peak radius curvature on the scale measurement.

We have decided to write an algorithm that simulates the stylus effect that we shall apply to the F_{MSCF} functions. By means of an inverse method, the scaling factor and the fractal dimension are adjusted to experimental data to reproduce profiles that look like the grinding profiles onto which the stylus scanning effect was simulated with a stylus radius curvature of 10 μm. Fig. 3c shows the simulated profile corresponding to the experimental one (Fig. 3a) including stylus integration simulation algorithm on original simulated profiles (Fig. 3b). Table 1 represents the usual roughness parameters on the experimental profiles, simulated profiles and stylus integration simulation algorithm profiles (Ra: mean roughness amplitude, Rt: range amplitude, peaks: number of peaks per inch, D: fractal dimension calculated by the average normalized autocorrelation method (ANAM) [24].

Table 1
Roughness parameters computation of profiles shown in Fig. 3

Roughness parameters	Experimental $r = 10$ (μm)	Simulated $r = 0$ (μm)	Simulated $r = 10$ (μm)
Ra	0.63	0.66	0.64
Rt	4.64	4.32	4.64
Peaks/inch	820	1186	814
Fractal dimension	1.08	1.23	1.09

The following remarks have to be made:

- Although our inverse method only calculated the two parameters (A, H) in Eq. (5), the experimental and simulated values of other roughness parameters are statistically equal (like peaks, Ra, etc.). We can therefore infer that:
  - o Our original fractal model is adequate to model some complex worn surfaces such as ground ones with only two parameters. Then the mechanism seems to be described by an amplitude phenomenon, a circle function basis, stochastic components and finally the fractal dimension.
  - o The fractal dimension estimation calculated by the ANAM seems very pertinent since estimated fractal dimension and theoretical fractal dimension given by H in Eq. (5) are equal as well as the frequency roughness parameters (peaks). The experimental profile then seems to be both Hölderian and anti-Hölderian since both the ANAM and the power law of the fractal peak radius curvature require these properties.
- The fractal dimension of a simulated profile with stylus integration is lower than the original simulated one because of a smoothing effect. This is also confirmed by the decrease in the number of peaks, characterizing a ‘less’ fractal profile.
- Amplitude parameters are quite constant (with a 10 μm stylus). The stylus effect does not fundamentally affect the amplitude parameter (however, the stylus radius should not be wide).

We then plot in Fig. 4, $\log r_c(l_x)$ versus $\log l_x$ for the three categories of profiles (in fact these are mean value of 30 profiles). The following remarks can be made:

- When $l_x > 30$ μm, all points are confounded in a linear log–log relation meaning that: (1) there is no quantified stylus effect, (2) experimental and simulated profiles are similar in a wide range of scales, (3) Hölderian and anti-Hölderian hypothesis on experimental profiles are respected.
- Both simulated stylus integration and experimental profiles present a step at the values of 10 μm, which is exactly the radius of curvature of the tip. Our method allows us to detect the stylus effect and more particularly, to quantify the radius of curvature of the profilometer. As a consequence, this method allows us to give the critical threshold on l_x and also l_y under which measurement effect can

affect a metric value constructed on the signal. This fact is a very important feature in the topographic measurement area.

- For the experimental profiles, if $l_x < 2$ μm the peak radius curvature increases linearly in log–log plot with l_x. This effect is related to the conversion from analogical to numerical mode that produces a white noise with low amplitude. Therefore, the method we have proposed allows us to detect high frequency components and also to quantify the amplitude range where measurement can be affected.

4. Conclusion

In this paper, we have proved that a process like grinding can be characterized with an elementary function and the worn profile can be modeled by a fractal curve defined by only two parameters (amplitude and fractal dimension) with an infinite summation of these elementary functions. Thanks to an inverse method and a multiscale characterization of the peak radius curvature of the profile, it was shown that the experimental profile was well modeled all over the scale. It was also shown that the fractal characterization allows us to find the scale where measurements become uncertain (in our cases the stylus integration) and to reconstruct the details that have been lost. However, to check if elementary functions well describe the process under study, we have to construct a method to measure the similarity of different profiles to verify if a given elementary function is better adapted than another. Using the theory of information, we are still working on this concept and results will soon be published.

Appendix A. The Fractal α-circle function

The aim of this appendix is to analyze the effect on the final modeled profiles by choosing a part of circle rather than half-circle one. Let us now define different circular functions represented on Fig. A1. To test the effects of the α angle on the profile shapes, 10 profiles with different angles and fractal dimensions Δ (varying from one to two) are simulated. Then two bivariate analyses of variance are processed on two roughness parameters to quantify the effect of both Ra (amplitude roughness parameter) and number of peaks per inch (frequency parameter). Fig. A2 and Fig. A3 represent, respectively, the α and Δ effects on Ra and the number of peaks, and Tables A1 and A2 represent their associated analyses of variance. Thanks to the Fisher test, it could be concluded that there is no effect of the α angle on both roughness parameters within a 5% error (on the contrary, fractal dimension gets a major influence on these parameters).

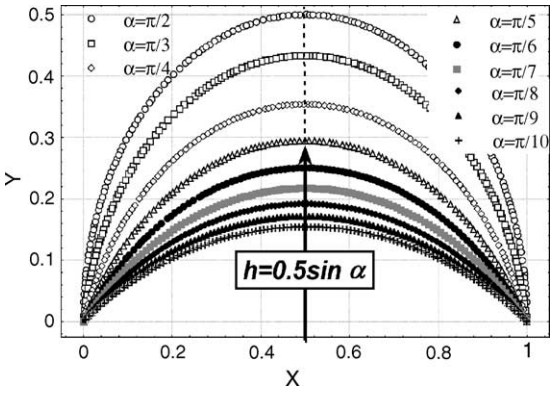

Fig. A1. Spectra of profiles with theoretical fractal dimension of 1.5 simulated by the Weierstrass function (left) and the circle function (right).

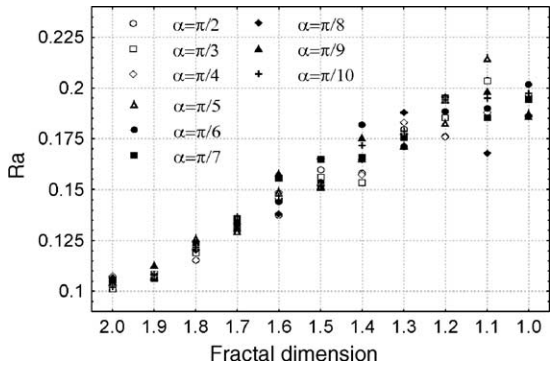

Fig. A2. Analyses of the circle angle (α) and the fractal dimension (Δ) effects on the Ra parameter.

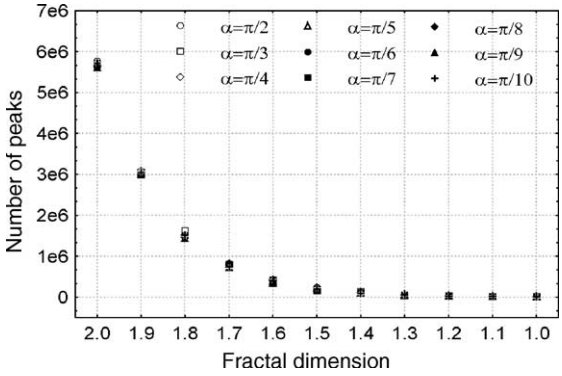

Fig. A3. Analyses of the circle angle (α) and the fractal dimension (Δ) effects on the number of peaks.

Appendix B. Comparison between the Weierstrass function and the circle function

The aim of this appendix is to compare the conventional Weierstrass function (WF) that is usually used to model the

Table A1
Analyses of variance to test the α effect, the fractal dimensions and their associated interaction ($\Delta \times \alpha$) on the Ra parameter

Ra	d.f. effect	MS effect	d.f. error	F	p_c-level
Δ	10	0.108801	990	258.4	0
α	8	0.000440	990	1.04	0.39
$\Delta \times \alpha$	80	0.000505	990	1.19	0.12

Table A2
Analyses of variance to test the α effect, the fractal dimensions and their associated interaction ($\Delta \times \alpha$) on the number of peak

Number of peaks	d.f. effect	MS effect	d.f. error	F	p_c-level
Δ	10	3.1538E + 14	990	22511	0
α	8	2.9248E + 10	990	2.08	0.05
$\Delta \times \alpha$	80	9119898624	990	0.65	0.99

roughness profiles with our circle function (CF). WF is defined by:

$$W(x) = A \sum_{n=0}^{+\infty} \phi_n \frac{\cos(2\pi\gamma^n x + \varphi_n)}{\gamma^{Hn}} \tag{B1}$$

with our functional circles given by Eq. (5). According to the fractal theory, the power density spectrum $P(s)$ (PDS) of both Weierstrass and circle functions present the following scaling law with the frequency f:

$$P(f) \propto \frac{1}{f^{2H+1}} \tag{B2}$$

As a consequence, the fractal dimension could be obtained by plotting in a log–log coordinate the relation between $P(f)$ and f, the slope a is then related to the fractal dimension by the relation:

$$\Delta(G_f) = \frac{5+a}{2} \tag{B3}$$

To compare the validity of our function, we shall simulate both WF and CF functions with a fractal dimension equal to 1.5. Then we shall analyze their related PDS. The aim is to show that usual WF is not well adapted to model the grinding process by the spectrum analysis. As can be observed in Fig. B1 (on the left), the WF PDS presents peaks of high amplitude (harmonics). These harmonics are related to the proper frequencies of each cos term in Eq. (B1). Experimental PDS do not present harmonics (carbide grain are deposited at random, no periodic vibration on the grinding machine, etc.). As a consequence, some artifacts will be present on the simulated profiles, which leads to a profile with heterogeneous amplitude observed at a given scale that does not correspond to the grinding profile. On the contrary, our CF PDS present in Fig. B1 (on the right) presents a continuous spectrum without any peaks. To well appreciate the accuracy of our modeling, we have calculated the fractal dimension of both spectra. For the WF profiles, we obtains $\Delta_{WF} = 1.334$ for a theoretical value of $\Delta_{Th} = 1.5$ that gives a systematic biased error of 17% (underestimation) on the fractal dimension. On the contrary, for CF, we obtain the value $\Delta_{CF} = 1.509$. It leads to an error lower than 1%, which is only due to stochastic variations (unbiased error) in the spectrum representation due to stochastic terms introduced in the CF definition.

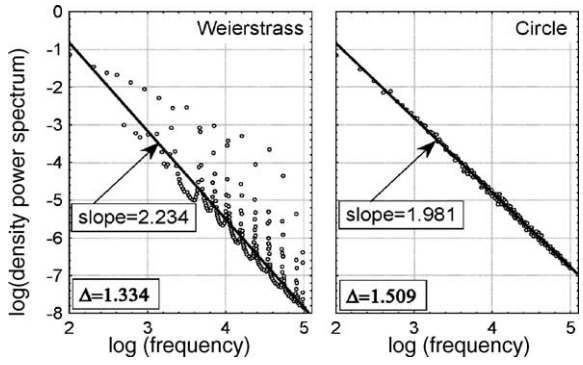

Fig. B1. Evolution of the $g(2^0x)$ function ($n = 0$) for different values of α ($\alpha = \pi/2$: half-circle, $\alpha = \pi/4$: quarter-circle, etc.).

Appendix C. A fractal definition of the local peak radius curvature

The curvature radius of a peak, r_c, for the fractal curves makes sense in terms of a scale when observed (Fig. C1). We postulate that the peak radius curvature can be defined on a given scale. We choose to calculate the value of r_c by the following method:

(1) We choose a horizontal line at the level h that crosses the profile. Then we calculate a set of l_x-values that cross the intercept line and the profile.
(2) For each l_x-value, the local maximal peak is computed and gives the l_y-value.
(3) The r_c is then computed from Eq. (C1). These operations are repeated for all the elements of the set of l_x-values

$$r_c(l_x) = \frac{l_x^2}{8l_y} \tag{C1}$$

(4) Another horizontal height is chosen and steps 1–3 are repeated.

Theorem. For all non constant continuous uniformly Hölderian and anti-Hölderian functions [23], f defined on

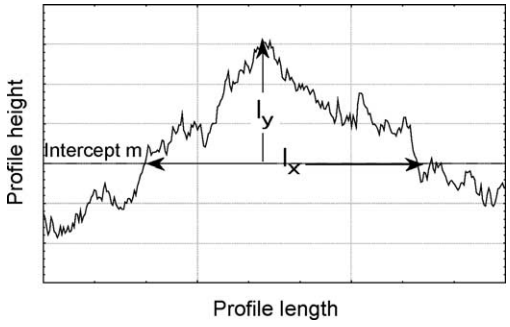

Fig. C1. Definition of l_x and l_y used to calculate the local peak radius curvature $r_c(l_x)$.

$[a, b]$, if l_x exists, then the fractal dimension of the profile is given by:

$$\Delta(G_f) = \limsup_{l_x \to 0} (\log r_c(l_x) / \log l_x) \quad \text{(C2)}$$

References

[1] D.J. Whitehouse, Digital techniques, in: T.R. Thomas (Ed.), Rough Surfaces, Longman, 1982, pp. 144–166.

[2] C.A. Brown, W.A. Johnsen, R.M. Butland, Scale-sensitive fractal analysis of turned surface, Ann. CIRP 45 (1996) 515–518.

[3] C.A. Brown, G. Savary, Describing ground surface texture using contact profilometry and fractal analysis, Wear 141 (1991) 211–226.

[4] M.O. Coppens, The effects of fractal surface roughness on diffusion and reaction in porous catalysts-from fundamentals to practical applications, Catalysis Today 53 (1999) 225–243.

[5] E. Doege, B. Laackman, B. Kischnick, Characterization of technical surfaces by means of fractal geometry, Steel Res. (1995) 113–116.

[6] E. Doege, B. Laackman, Fractal geometry used for the characterization of sheet surfaces, Ann. CIRP 44 (1995) 197–200.

[7] J.J. Gagnepain, C. Roques-Carmes, Fractal approach to two-dimensional and three-dimensional surface roughness, Wear 109 (1986) 119–126.

[8] M. Hasegawa, J. Liu, K. Okuda, Calculation of the fractal dimension of machined surface profiles, Wear 192 (1996) 40–45.

[9] B.B. Mandelbrot, The Fractal Geometry of Nature, W.H. Freeman and Company, New York, 1983.

[10] B.B. Mandelbrot, Les Objets Fractals, Flammarion, Paris, 1975.

[11] B. Dubuc, J.F. Quiniou, C. Roques-Carnes, C. Tricot, S.W. Zucker, Evaluating the fractal dimension of profiles, Phys. Rev. A 39 (3) (1989) 1500–1512.

[12] C. Tricot, Courbes et Dimension Fractale, Springer-Verlag, Paris, 1993.

[13] D. Whebi, Approche fractale de la rugosité des surfaces et implication analytique, Ph.D. Thesis, Besançon, France, 1986.

[14] J. Lopez, G. Hansali, J.C. Le Bossa, T. Mathia, Caractérisation fractale de la rugosité tridimensionnelle d'une surface, J. Phys. III 4 (1994) 2501–2519.

[15] S. Ganti, B. Bushan, Generalized fractal analysis and its applications to engineering surfaces, Wear 180 (1995) 17–34.

[16] B.B. Mandelbrot, J.W. Van Ness, Fractional Brownian motions, fractional noises and applications, SIAM Rev. 10 (1968) 422–437.

[17] B.B. Mandelbrot, J.R. Wallis, Computer experiments with fractal Gaussian noises. Part 1, averages and variances, Water Resour. Res. (1969) 228–241.

[18] C.Y. Poon, B. Bhusham, Comparison of surface roughness measurements by stylus profiler, AFM, and non-contact optical profiler, Wear 190 (1995) 76–88.

[19] J.I. Mc Cool, Comparison of models for the contact of rough surfaces, Wear 107 (1986) 37–60.

[20] V. Radhakrishnan, Effect of stylus radius on the roughness values measured with tracing stylus instruments, Wear 16 (1970) 325–335.

[21] D.J. Whitehouse, Theoretical analysis of stylus integration, Ann. CIRP 23 (1974) 181–182.

[22] T. Nakamura, On deformation of surface roughness curves caused by finite radius of stylus tip and tilting of stylus holder arm, Bul. Jpn. Soc. Precision Eng. 1 (1966) 240–248.

[23] M. Bigerelle, Caractérisation géométrique des surfaces et interfaces: applications en métallurgie, Ph.D. Thesis, Ecole Nationale Supérieure d'Arts et Métiers, Lille, France, 1999.

[24] M. Bigerelle, A. Iost, Calcul de la dimension fractale d'un profil par la méthode des autocorrélations moyennées normées A.M.N, C. R. Acad. Sci. Paris 323 (1996) 669–675.